Am J Cancer Res 2026;16(5):1776-1790
www.ajcr.us /ISSN:2156-6976/ajcr0172961

Original Article

Paeonol inhibits prostate cancer progression via the miR-145-5p/GOLM1 axis

Yingxin Zhang

College of Life and Environmental Sciences, Minzu University of China, Beijing 100081, China

Received March 29, 2026; Accepted May 8, 2026; Epub May 15, 2026; Published May 30, 2026

Abstract: Paeonol, derived from *Paeonia suffruticosa*, is a potent ingredient known for its diverse benefits such as anti-tumor, antioxidant, and cardiovascular system protection. Currently, there is uncertainty about the impact of paeonol on prostate cancer (PCa). This research aims to explore how paeonol affects the PCa development and its specific mechanism. To screen the optimal concentration, the impact of paeonol on cell viability was examined via Cell Counting Kit-8 assay. The biological behaviors of PCa cells were evaluated via multiple approaches, including colony formation, Transwell, wound healing assay, and flow cytometry. MiR-145-5p level in PCa cells was assessed using quantitative real-time polymerase chain reaction (qRT-PCR), subsequently explored the impact of miR-145-5p overexpression on the biological properties of PCa cells. Bioinformatics analysis predicted the downstream target mRNA of miR-145-5p, while the dual-Luciferase reporter gene assay confirmed the targeting connection between the two. A subcutaneous xenograft tumor model was established to explore how paeonol may impact tumor growth by modulating miR-145-5p/Golgi membrane protein 1 (GOLM1). Results showed that Paeonol exerted suppressive effects on the malignant biological properties of PCa cells, along with induced apoptosis. PCa cells exhibited lower miR-145-5p level as opposed to normal cells, and paeonol treatment up-regulated miR-145-5p. GOLM1 was highly expressed in PCa cells, while miR-145-5p could directly target and downregulate GOLM1 expression. miR-145-5p overexpression suppressed the malignant biological properties of PCa cells, but GOLM1 overexpression reversed this effect. Silencing of miR-145-5p or GOLM1 overexpression both weakened the anti-tumor impacts of paeonol. Additionally, tumor growth was suppressed and apoptosis was induced in tumor cells *in vivo* by paeonol. In conclusion, Paeonol suppresses the malignant progression of PCa, and promotes cell apoptosis via regulating the miR-145-5p/GOLM1 axis.

Keywords: Prostatic cancer, paeonol, miR-145-5p, Golgi membrane protein 1, invasion, apoptosis

Introduction

According to the latest statistical analysis in USA, more than 313,780 new cases of Prostate cancer (PCa) are expected to occur in 2025, leading the list of malignant tumors in men, and more than 35,000 new deaths [1]. In the early stages of PCa, the progression could be effectively controlled by surgical resection and radiotherapy [2-4]. However, recurrence or metastasis after radical prostatectomy occurs in about 30% of patients, whereas for these individuals, androgen deprivation therapy (ADT) remains the main clinical strategy, typically including gonadotropin-releasing hormone agonists or surgical gonadectomy [5]. However, the majority of patients deteriorate again after 10-15 months of ADT, and the tumor is no longer affected by the body's androgen levels, transforming into castration-resistant prostate cancer [6, 7]. Once progressed to this stage, the patient's therapeutic space will be very limited and the mortality rate will increase dramatically [8, 9]. Therefore, in-depth investigate the mechanisms of PCa progression and search for novel and efficient treatment options are particularly important for the management of PCa patients.

Researchers are increasingly focused on the anti-tumor properties of herbal extracts because of their excellent safety profile, minimal toxic effects, and ability to target multiple pathways [10, 11]. Paeonol, the main bioactive constituent isolated from the dried root bark of *Paeonia suffruticosa*, which has a wide range of antioxidant, neurological and cardiovascular

https://doi.org/10.62347/YNVE5413

system protection effects [12-14]. Notably, paeonol has shown excellent inhibitory effects on several types of cancers, including lung [15], pancreatic [16], and ovarian [17]. Paeonol can achieve anti-tumor effects by mediating multiple signaling pathways and targets, and can effectively rise the sensitivity of cancer cells to chemotherapy and radiotherapy [18, 19]. Previous study has shown that paeonol induces apoptosis in HeLa cervical cancer cells through the Phosphatidylinositol 3-Kinase/AKT Serine pathway, and causes mitochondrial dysfunction, demonstrating its potential for the treatment of cervical cancer [20]. However, while paeonol has shown promise in other cancer types, its specific role and molecular mechanism in regulating the malignant progression of PCa are poorly understood.

With approximately 20-24 nucleotides in size, microRNAs (miRNAs) are involved in controlling gene expression in plants and animals at the post-transcriptional level [21, 22]. Numerous studies have indicated that abnormal miRNA expression is linked to the pathological processes of various cancers, and miRNAs can function as either tumor suppressors or oncogenes [23, 24]. Positioned on chromosome 5 (5q32), miR-145-5p is transcribed from the MIR145 in the human genome [25]. Existing studies have indicated that miR-145-5p acts as an anticancer factor in various cancers, like pancreatic cancer [26] and breast cancer [27]. Notably, miR-145-5p is reduced in tumor tissues from individuals with PCa bone metastases, implying that low miR-145-5p level serves as an indicator of PCa metastasis and invasion [28]. At present, the specific action mechanism of miR-145-5p in regulating PCa malignant progression remains poorly understood.

Expressed mainly in epithelial cells, Golgi membrane protein 1 (GOLM1) is associated with tumor development, metastasis, and immunosuppression, and has emerged as a new focus in cancer research in recent years [29]. A recent study revealed that GOLM1 drives epithelial mesenchymal transition in PCa cells and is a key oncogene in PCa malignant development [30]. We discovered that GOLM1 is a potential target mRNA of miR-145-5p through bioinformatics analysis. On this basis, we postulated that paeonol could suppress PCa progression through modulating miR-145-5p/GOLM1 axis. Based on this postulation, this research was designed to explore the influence of paeonol, miR-145-5p or GOLM1 overexpression on the malignant properties of PCa cells. Additionally, to investigate the impact of paeonol on tumor growth, we established a mouse model with subcutaneously transplanted tumors. This study is the first to investigate the link between paeonol and the miR-145-5p/GOLM1 axis, and aims to elucidate the specific mechanisms by which paeonol inhibits PCa progression, so as to provide a novel theoretical basis and experimental evidence for the clinical translation of paeonol in the treatment of PCa.

Materials and methods

Cell culture

Human normal prostate epithelial cells RWPE1 (SNL-569), PCa cells LNCaP (SNL-356) and C4-2 (SNL-160) were obtained from Sunncell Biotechnology (Hubei, China). Before testing, the culture of RWPE-1 cells was carried out in Keratinocyte-SFM medium (17005042, Invitrogen, Carlsbad, CA, USA). Meanwhile, PCa cells were grown in a mixture of 1640 complete medium (SNM-001E, Sunncell Biotechnology) at 37°C with 5% CO_2 (v/v).

Cell counting kit-8 (CCK-8) assay

LNCaP and C4-2 cells were plated in 96-well plates (1.5×10^4/well) and left to culture for 24 h. After the cell adhesion, 200 μL of medium containing paeonol (0, 5, 10, 20, 40, or 80 μg/mL, A423049, Sangon Biotech, Shanghai, China) was dispensed into each well [31]. After treatment for 48 h, 20 μL of CCK-8 reagent (C917226, Macklin Inc., Shanghai, China) was introduced. After a 2-hour incubation under the condition of avoiding light, to screen the optimal concentration of paeonol, the optical density $(OD)_{450}$ values of the cells were determined.

Cell transfection

miR-145-5p mimic (mimic), miR-145-5p inhibitor (inhibitor), GOLM1 overexpression plasmid (OE-GOLM1, without the 3'UTR of GOLM1 mRNA), or negative control (mimic NC, inhibitor NC, and OE-NC) were obtained by Sangon Biotech. The seeding density for LNCaP and C4-2 cells in 24-well plates was set at 1×10^4

cells/well. At 50%-60% cell confluence, transfection was performed using Lipofectamine 3000 reagent (L3000150, Invitrogen) for 48 h. Subsequently, miR-145-5p and GOLM1 levels was analyzed to evaluate the transfection efficiency.

Colony formation assay

LNCaP and C4-2 cells were taken, phosphate buffer saline (PBS)-washed, digested with 0.25% trypsin (T917499, Macklin Inc.). The cells were then plated into 6-well culture plate (500 cells/well), and incubated for 14 days at 37°C. The culture medium with or without paeonol was changed every 2-3 d. Cell culture was terminated once visible cell colonies had formed. The culture supernatant was removed, fixation was performed by adding 4% paraformaldehyde (P885233, Macklin Inc.) for 30 min. The fixative was then removed, and cells were exposed to crystal violet (A600331, Sangon Biotech) for 10 min. Cells were viewed using a microscope (CX33, Olympus, Tokyo, Japan), and the colony formation rate was subsequently calculated.

Wound healing assay

1 mL of LNCaP and C4-2 cell suspension (3×10^5 cells/mL) was placed in 6-well cell culture plates. After the cells were fully adherent and grown to approximately 90% confluence, the culture medium was removed, and a sterile 20 μL pipette tip was employed to produce a straight line and evenly in the center of the cell monolayer. The detached cells in the scratched region were gently washed off with PBS, and the serum-free medium containing 5 μg/mL mitomycin C (HY-13316, MedChemExpress, Monmouth Junction, NJ, USA) was introduced to the wells and incubated for 2 h at 37°C. The medium containing mitomycin C was discarded, and then the medium containing 40 μg/mL paeonol was added, and the scratch width was immediately photographed under a microscope and recorded as 0 h. After 24 h, the width of the scratch was assessed with ImageJ software (National Institute of Mental Health, USA), so as to determine the cell migration ability.

Transwell assay

Prior to experimentation, Matrigel matrix gel (356234, Corning, MA, USA) was thawed overnight at 4°C, and then diluted with serum-free medium in a 1:8 proportion. The diluted mixture (100 μL) was introduced to the upper chamber of each Transwell insert (Corning) at 37°C for 2 h. 200 μL of LNCaP or C4-2 cell suspension (5×10^4 cells/mL, resuspended in serum-free medium) was plated into the upper section, and complete medium (600 μL) was placed in the lower chamber. After a 24-hour incubation, the non-invading cells on the membrane surface were gently removed with a cotton swab. Subsequently, the invaded cells were fixed in 4% paraformaldehyde for 25 min, and then dyed with 0.1% crystal violet staining solution. Five random fields per insert were captured under a microscope, and the number of invasive cells was quantified using ImageJ software.

In the Transwell migration assay, Matrigel was not needed in the Transwell chamber, and other procedures were consistent with the invasion assay.

Flow cytometry

Following various treatments, PCa cells were gathered, and then mixed with 500 μL of 1× Binding Buffer (C1062S, Beyotime). Subsequently, Annexin V-Fluorescein Isothiocyanate (FITC) reagent (5 μL) and propidium iodide (PI) solution (5 μL) were added into the cell suspension at 25°C in darkness for 15 min. After washing with Annexin V Binding Buffer, the apoptosis rate of PCa cells was detected and quantitatively analyzed using a flow cytometer (BD FACSCalibur™, BD Biosciences, CA, USA).

Bioinformatics analysis

To identify the potential target genes of miR-145-5p, we conducted bioinformatic analysis utilizing Gene Expression Profiling Interactive Analysis (GEPIA) (http://gepia.cancer-pku.cn/), miRWalk (http://mirwalk.umm.uni-heidelberg.de/), and miRDB (https://mirdb.org/) databases. Candidate target genes that were screened from the three databases were subsequently subjected to intersection analysis, and GOLM1 was ultimately identified as the core target gene of miR-145-5p.

Dual-luciferase reporter assay

Dual-luciferase reporter plasmids targeting the 3' untranslated region (3'UTR) of GOLM1,

including wild-type (Wt) and mutant (Mut) versions, were synthesized by Sangon Biotech. Utilizing the Lipofectamine 3000, GOLM1 Wt and mimic NC, GOLM1 Wt and mimic, GOLM1 Mut and mimic NC, GOLM1 Mut and mimic were co-transfected into PCa cells, respectively. Following a 48-hour incubation period, cells were gathered and the luciferase activity of PCa cells was assessed utilizing the Double-Luciferase Reporter Assay Kit (E608006, Sangon Biotech).

Subcutaneous tumor model in nude mice

Male BALB/c nude mice (14-18 g, 4-6 weeks old), were acquired from Vitalriver (Beijing, China) and housed at 22°C with 45%-55% relative humidity. LNCaP cells (untransfected, or transfected with miR-145-5p inhibitor or inhibitor NC) were resuspended in a pre-cooled mixture of serum-free 1640 medium and Matrigel matrix gel at a 1:1 volume ratio. After a 7-day acclimatization period, each mouse received a single subcutaneous injection of 100 µL cell suspension (1×10^5 cells/each) into the right axilla. One week later, the mice injected with untransfected LNCaP cell suspension were randomly divided into the control group (0.3 mL normal saline daily via intraperitoneal injection) and the paeonol-treated group (50 mg/kg/d paeonol daily via intraperitoneal injection) using a random number table; mice injected with LNCaP cell suspension transfected with inhibitor NC or inhibitor were divided into the paeonol+inhibitor NC group and paeonol + miR-145-5p inhibitor group (both received 50 mg/kg/d paeonol daily) (n=6). All animals received daily intraperitoneal injections for 14 days. Tumor dimensions were monitored daily using vernier calipers, and tumor volume was then calculated. After the last administration, mice were anesthetized by inhalation of isoflurane (3%), and euthanization by cervical dislocation. Tumor tissues were fully excised using tissue scissors, and photographed for recording.

Quantitative real-time polymerase chain reaction (qRT-PCR)

Total RNA was isolated from RWPE1, LNCaP, C4-2 cells and tumor tissues via TRIzol reagent (15596026, Invitrogen). Subsequently, complementary DNA (cDNA) was synthesized by reverse transcription using AMV reverse transcriptase (2621, TAKARA, Tokyo, Japan). Using the prepared cDNA as the amplification template, PCR was carried out with TB Green FAST qPCR kit (CN830S, TAKARA) to detect the levels of target genes. The 25 µL qRT-PCR reaction system was configured as follows: 12.5 µL TB Green FAST qPCR Mix, 1 µL forward primer (0.4 µM), 1 µL reverse primer (0.4 µM), 2.5 µL cDNA template, and 8 µL RNase-free water. The qRT-PCR reaction conditions were set as: predenaturation at 95°C for 30 s; followed by 40 cycles of denaturation at 95°C for 5 s and annealing/extension at 60°C for 30 s; finally, melting curve analysis was performed to verify the specificity of amplification. U6 and GAPDH were separately employed as the internal reference genes for miR-145-5p and GOLM1, respectively. The relative expression level of target genes was calculated using the $2^{-\Delta\Delta Ct}$ method.

Primer sequences utilized in this experiment: miR-145-5p: F: 5'-TGTCCAGTTTTCCCAGGAATC-3'; R: 5'-CTCAACTGGTGTCGTGGAGTC-3'. U6: F: 5'-CTGGTGAAGGGGAGGGGATA-3'; R: 5'-ACAGGATAGGGGGACCACTC-3'. GOLM1: F: 5'-CCGGAGCCTCGAAAAGAGAT-3'; R: 5'-CTGCTGTCTCTGGTCGTTGT-3'. GAPDH: F: 5'-TCGGCAGGATGTAGGGCTAAAAGC-3'; R: 5'-GTAGCCCATGGGTTTTAGCCC-3'.

Terminal deoxynucleotidyl transferase dUTP nick end labeling (TUNEL) staining

Excised tumor tissues were fixed in paraformaldehyde (4%, w/v) for 24 h at room temperature, and then dehydrated through a graded ethanol series. After that, tumor tissues were embedded in paraffin and sectioned (5 µm thick), dewaxed using xylene (X820584, Macklin), and then rehydrated through a graded ethanol series. The sections were incubated with 20 µg/mL of Proteinase K (DNase-free, ST532, Beyotime) for 30 min at 25°C, and then covered with TUNEL assay solution (C1086, Beyotime) at 37°C for 60 min in darkness. The sections were then counterstained with 4',6-diamidino-2-phenylindole (DAPI) solution (C1005, Beyotime) for 10 min in the dark, and then imaged under a fluorescence microscope.

Immunohistochemistry

Tumor tissue sections were dewaxed using xylene, rehydrated through a graded ethanol

series, and then subjected to antigen retrieval via microwave irradiation in sodium citrate buffer. After that, they were placed in 3% H_2O_2 solution for 30 min, then rinsed thoroughly with PBS, and blocked with 5% bovine serum albumin (BSA, A351835, Sangon Biotech) for 30 min. After incubating the sections at 37°C with primary antibody Ki67 (ab21700, prediluted, Abcam, MA, USA) for 90 min, they were incubated with goat anti-rabbit IgG (31466, 1:500, Invitrogen) for 30 min in darkness at 25°C. Color development was performed using 3,3'-Diaminobenzidine (DAB) solution (E670035, Sangon Biotech), and the reaction was terminated with distilled water. The sections were restained with hematoxylin solution (H913272, Macklin) for 3 min, mounted with neutral balsam (N861409, Macklin), and then viewed with an optical microscope.

Western blot

RWPE1 cells, PCa cells, and mouse tumor tissues were fully lysed with Radio immunoprecipitation assay lysate buffer (P0013B, Beyotime) to extract proteins, and protein concentrations were quantified using the Bicinchoninic Acid (BCA) Assay kit (P0012, Beyotime). Following protein separation was completed by gel electrophoresis, the proteins were transferred to Polyvinylidene Fluoride membranes (Invitrogen), which were blocked for 3 h using 5% BSA. The membranes were treated overnight with primary antibody GOLM1 (PA5-30622, 1:2000, Invitrogen) at 4°C. After being rinsed with Tris-Buffered Saline Tween-20 (TBST), membranes were incubated with goat anti-rabbit IgG (31466, 1:5000, Invitrogen) for 2 h. Enhanced Chemiluminescence working solution (34577, Invitrogen) was evenly applied to the membranes, and then scanned using an Amersham ImageQuant™ 800 gel imaging system (Cytiva, Shanghai, China). The gray intensity of each protein band was analyzed via ImageJ software, with Glyceraldehyde-3-Phosphate Dehydrogenase (GAPDH) (MA5-15738, 1:1000, Invitrogen) as an internal reference.

Statistical analysis

Each independent experiment was conducted with a minimum of three biological replicates, and results were presented as the mean ± standard deviation. Figures were drawn with Prism software (GraphPad 9.0), and statistical analyses were conducted using SPSS 26.0 (IBM SPSS Statistics). Student's *t*-test was employed to evaluate differences between two groups. For comparisons among multiple groups, one-way ANOVA followed by Tukey's post-hoc multiple comparison test was performed. For comparisons among multiple groups with time-dependent variables (tumor volume monitored at consecutive time points), repeated measures ANOVA was applied, followed by Bonferroni post-hoc test for pairwise comparisons between groups. One-way ANOVA was performed. *$P<0.05$ was considered significant difference.

Results

Paeonol inhibits malignant biological properties of PCa cells

Following different doses of paeonol treated for 48 h, both 40 and 80 μg/mL of paeonol treatment caused a marked decrease in cell viability, with the impact increasing with higher doses (**Figure 1A**, **1B**). Paeonol at 40 μg/mL had already shown a significant suppressive effect on cell viability, we determined this concentration of paeonol as suitable for the subsequent studies. The colony formation experiment results indicated that the colony formation rate of PCa cells was significantly decreased after paeonol treatment (**Figure 1C**). After treatment with paeonol, cell migration rate of PCa cells was notably reduced (**Figure 1D**). Transwell assay results showed that the number of migratory and invasive LNCaP and C4-2 cells was also reduced after paeonol treatment (**Figure 1E**, **1F**). In addition, paeonol treatment resulted in markedly higher apoptosis rates (**Figure 1G**). These findings indicated that paeonol treatment effectively inhibited the malignant biological properties of PCa cells.

Paeonol up-regulates miR-145-5p in PCa cells

miR-145-5p expression in LNCaP, C4-2, and RWPE1 cells was examined via RT-qPCR. There was a notable difference in miR-145-5p level between LNCaP, C4-2, and RWPE1 cells, with RWPE1 cells exhibiting higher levels (**Figure 2A**). Not only that, following paeonol treatment, miR-145-5p expression showed a notable increase in PCa cells, indicating that paeonol up-regulates miR-145-5p level (**Figure 2B**, **2C**). To investigate the role of miR-145-5p overex-

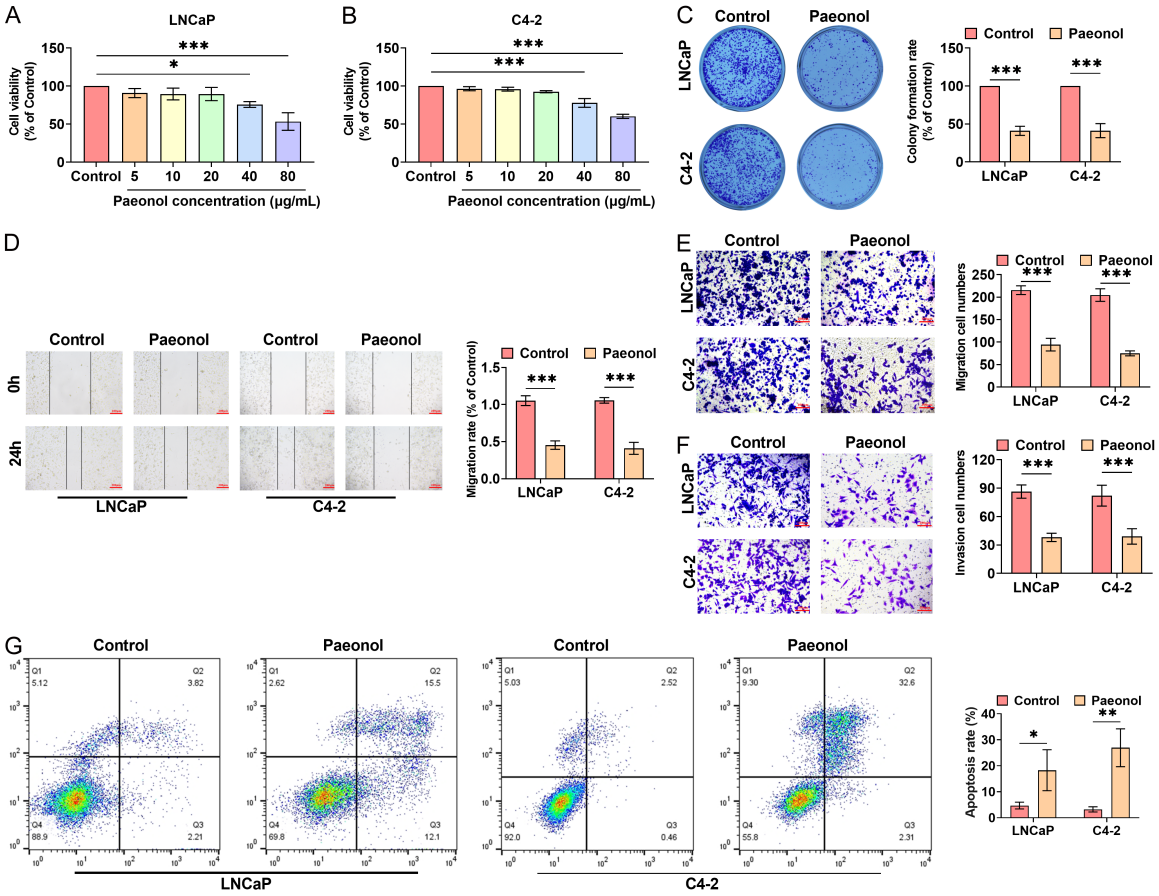

Figure 1. Paeonol inhibits malignant biological properties of PCa cells. A, B. CCK-8 assay was performed to examine the viability of PCa cells, to screen the optimal concentration of paeonol treatment. C. Colony formation assay was used to evaluate the impact of 40 μg/mL of paeonol treatment on colony formation rate. D. Wound healing assay determined migration after paeonol treatment, and the cell migration rate was subsequently computed (10×, 200 μm). E, F. Cell migration and invasion abilities of cells were examined using Transwell assay (20×, 100 μm). G. Annexin V-FITC/PI assay was performed to detect the apoptosis rate after paeonol treatment. PCa: Prostate Cancer; CCK-8: Cell Counting Kit-8; PI: Propidium Iodide; FITC: Fluorescein Isothiocyanate. (*P<0.05, **P<0.01, ***P<0.001).

pression on cell malignant biological properties, we transfected mimic in PCa cells. After transfection with miR-145-5p mimics, miR-145-5p level was notably upregulated in PCa cells, indicating a high transfection efficiency and its suitability for subsequent experiments (**Figure 2D**). miR-145-5p overexpression notably reduced the colony formation rate (**Figure 2E**) and migration rate (**Figure 2F**) of PCa cells. Furthermore, transfection with miR-145-5p mimics resulted in a decline in the number of migratory and invasive cells (**Figure 2G**, **2H**), as well as an increase in apoptosis rate (**Figure 2I**). Altogether, these outcomes indicated that miR-145-5p is up-regulated by paeonol, and miR-145-5p overexpression suppresses PCa malignant biological behaviors, suggesting that paeonol may exert its inhibitory effect on PCa malignant biological behaviors by up-regulating miR-145-5p.

miR-145-5p directly targets and negatively regulates GOLM1

To delve into the specific mechanism underlying the inhibition of PCa malignant biological behaviors by up-regulating miR-145-5p, bioinformatic prediction of the downstream target mRNAs of miR-145-5p was carried out. After analyzing the overlapping candidate genes from the three datasets, GOLM1 was ultimately screened out as the key target gene (**Figure 3A**). Additionally, the direct binding sequence between miR-145-5p and the 3'UTR region of GOLM1 was acquired from the miRWalk database (**Figure 3B**). Based on the analysis of the

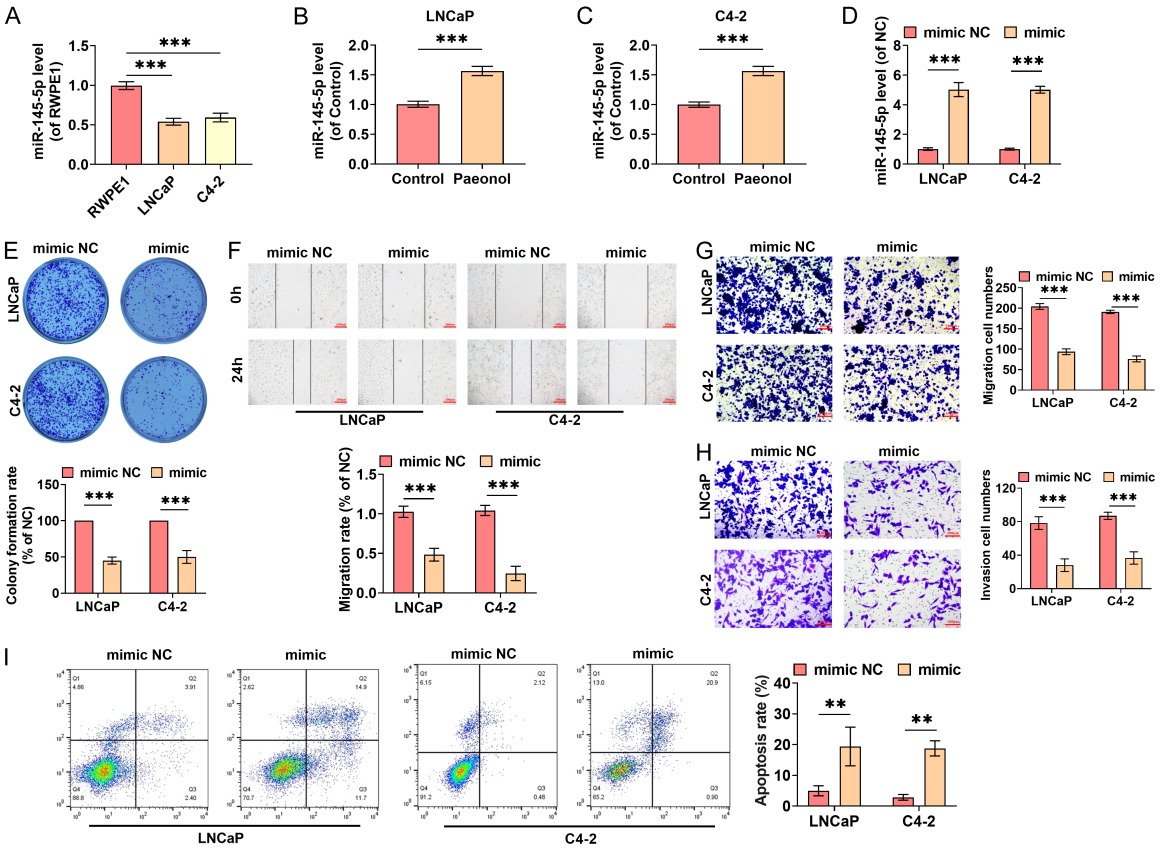

Figure 2. Paeonol up-regulates miR-145-5p in PCa cells. A. qRT-PCR was performed to detect miR-145-5p level in RWPE1, LNCaP and C4-2 cells. B, C. RT-qPCR was used to analyze miR-145-5p level following a 48-hour exposure to 40 μg/mL paeonol in LNCaP and C4-2 cells. D. MiR-145-5p level was analyzed by qRT-PCR to validate the transfection efficiency. E. Colony formation assay was performed to evaluate the colony formation rate of cells after transfected with mimic NC or mimic. F. Following transfection, cell migration rate was determined via wound healing assay (10×, 200 μm). G, H. Transwell was performed to assess the number of migratory and invasive cells after transfection (20×, 100 μm). I. Annexin V-FITC/PI assay detected the apoptosis rate after transfection. PCa: Prostate Cancer; qRT-PCR: Quantitative Real-Time Polymerase Chain Reaction; PI: Propidium Iodide; FITC: Fluorescein Isothiocyanate. (***P*<0.01, ****P*<0.001).

GEPIA database, GOLM1 level was markedly elevated in PCa in comparison to normal tissues (**Figure 3C**). To further validate the targeted interaction between miR-145-5p and GOLM1, a dual-luciferase reporter assay was performed. miR-145-5p overexpression evidently reduced the luciferase activity of GOLM1 Wt, but no significant alteration was detected in the Mut group, suggesting that GOLM1 is a direct downstream target of miR-145-5p (**Figure 3D**, **3E**). Furthermore, overexpression of miR-145-5p significantly reduced the protein level of endogenous GOLM1, while inhibition of miR-145-5p markedly upregulated endogenous GOLM1 protein expression in both LNCaP and C4-2 cell lines, indicating that miR-145-5p had a negative regulatory impact on GOLM1 (**Figure 3F**). Additionally, GOLM1 expression was notably higher in PCa cells (LNCaP and C4-2) than in normal cells (RWPE1), which was consistent with the expression trend revealed by the GEPIA database (**Figure 3G**, **3H**).

GOLM1 overexpression partially attenuates the suppressive impact of miR-145-5p overexpression on the malignant phenotypes of PCa cells

To investigate the influence of GOLM1 overexpression on PCa cells, we transfected PCa cells with OE-GOLM1 and determined its overexpression efficiency. After PCa cells were transfected with OE-GOLM1, GOLM1 mRNA and protein levels in PCa cells were notably upregulated, which

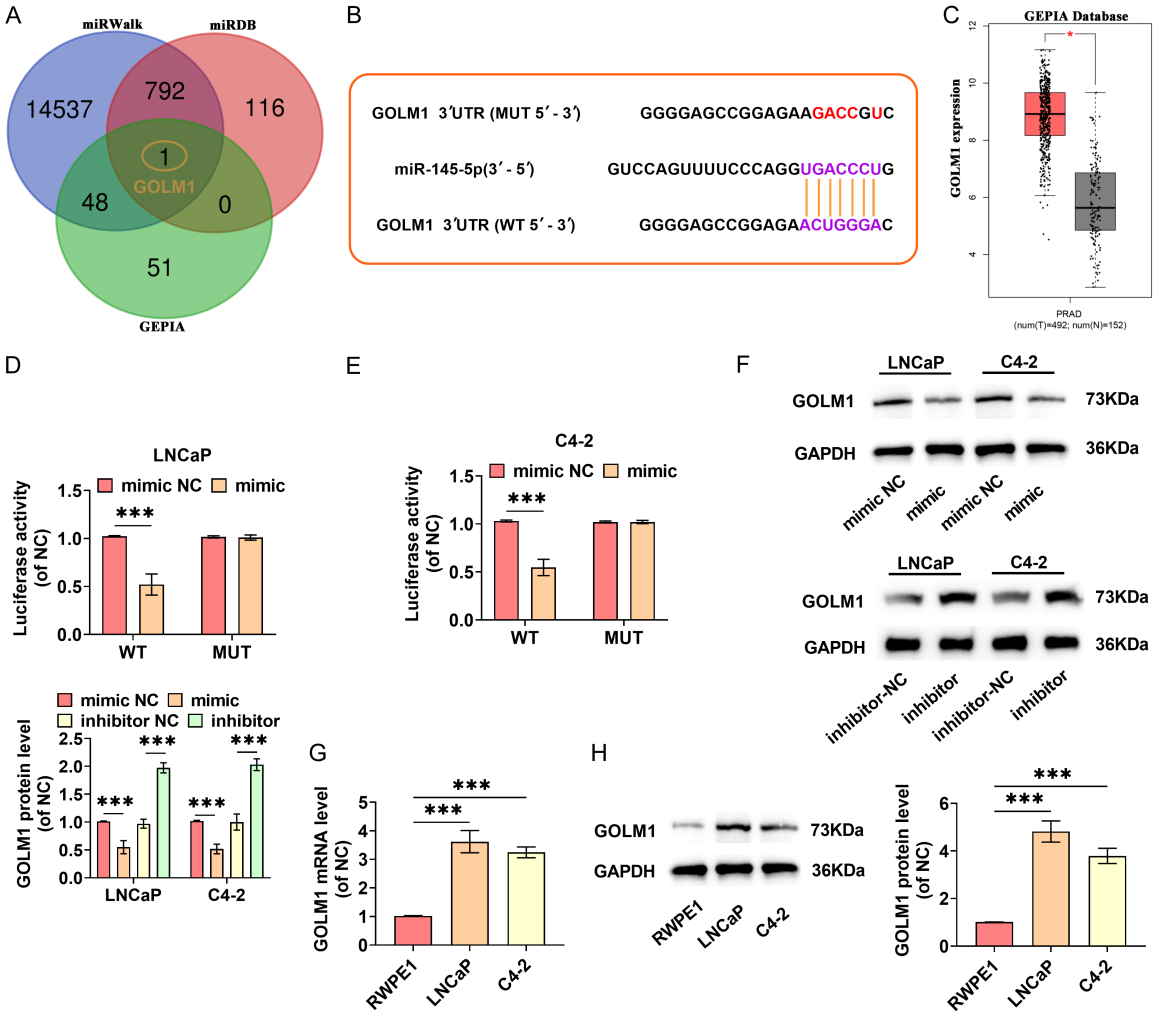

Figure 3. GOLM1 is regulated by miR-145-5p, causing its downregulation. A, B. miRWalk, miRDB and GEPIA databases predicted the target mRNA of miR-145-5p, and the binding site between miR-145-5p and GOLM1 was predicted via miRWalk database. C. Analysis based on the GEPIA database showed that GOLM1 was highly expressed in PCa tissues. D, E. Dual-Luciferase reporter assay was performed to verify miR-145-5p directly targets and negatively regulates GOLM1. F. Western blot was performed to detect the level of GOLM1 protein after transfection with mimic/mimic NC or inhibitor/inhibitor NC. G, H. The levels of GOLM1 in RWPE1, LNCaP and C4-2 cells were detected via qRT-PCR and Western blot. GOLM1: Golgi Membrane Protein 1; GEPIA: Gene Expression Profiling Interactive Analysis; PCa: Prostate Cancer; qRT-PCR: Quantitative Real-Time Polymerase Chain Reaction. (***P<0.001).

satisfied the requirements of subsequent experiments (**Figure 4A**, **4B**). We noticed that GOLM1 overexpression weakened the suppression of miR-145-5p overexpression on colony formation in LNCaP and C4-2 cells (**Figure 4C**). Furthermore, GOLM1 overexpression also weakened the suppression of miR-145-5p overexpression on cell migration and invasion (**Figure 4D**, **4E**). GOLM1 overexpression impaired the pro-apoptotic effect of miR-145-5p overexpression (**Figure 4F**). Taken together, the inhibitory effects of miR-145-5p overexpression on cell colony formation, migration, invasion of PCa cells was weakened by GOLM1 overexpression, suggesting that miR-145-5p exhibited its anti-tumor effect by downregulating GOLM1.

Paeonol inhibits malignant phenotypes of PCa cells by modulating the miR-145-5p/GOLM1 axis

After PCa cells were transfected with miR-145-5p inhibitor, miR-145-5p level was notably decreased, which confirmed the successful transfection of the inhibitor (**Figure 5A**).

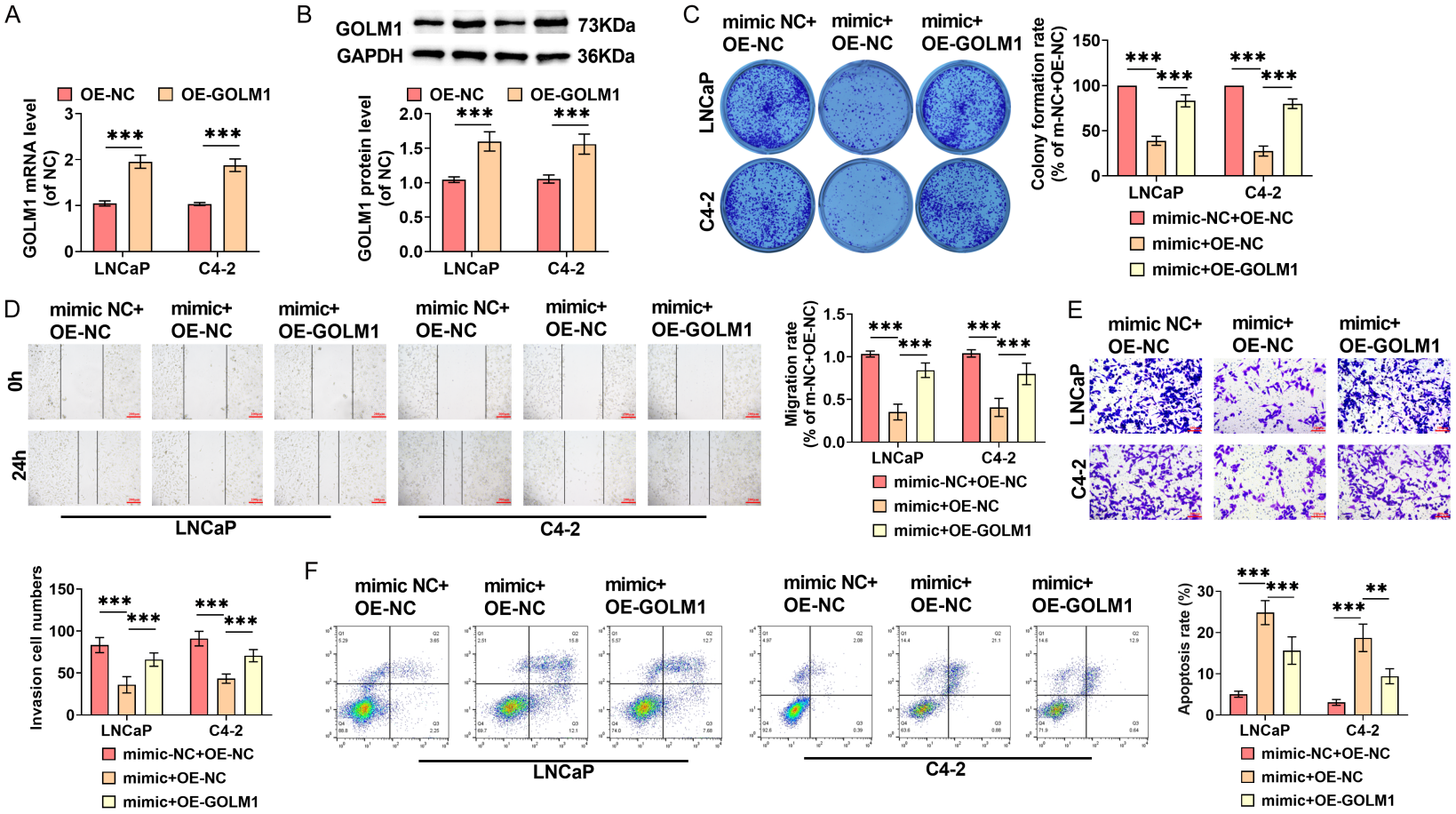

Figure 4. GOLM1 overexpression partially attenuates the suppressive effects of miR-145-5p overexpression on malignant phenotypes of PCa cells. A. After transfection with OE-NC or OE-GOLM1, qRT-PCR was performed to quantify the mRNA level of GOLM1 to verify transfection efficiency. B. Western blot was performed to detect the level of GOLM1 protein after transfection. C. Colony formation assay was used to evaluate cell colony formation rate after transfection. D. Wound healing assay was performed to detect the migration ability of PCa cells after transfection (10×, 200 μm). E. Transwell assay was performed to examine cell invasion after transfection with OE-NC or OE-GOLM1 (20×, 100 μm). F. Annexin V-FITC/PI assay detected the apoptosis rate. PCa: Prostate Cancer; qRT-PCR: Quantitative Real-Time Polymerase Chain Reaction; PI: Propidium Iodide; FITC: Fluorescein Isothiocyanate. (***P*<0.01, ****P*<0.001).

Paeonol treatment led to a notable reduction in GOLM1 expression, whereas silencing of miR-145-5p or GOLM1 overexpression both caused a marked increase in GOLM1 expression, suggesting that paeonol could regulate the miR-145-5p/GOLM1 axis (**Figure 5B**, **5C**). Paeonol treatment markedly reduced the colony formation rate (**Figure 5D**) and migration rate (**Figure 5E**) of PCa cells, whereas silencing of miR-145-5p or GOLM1 overexpression both weakened the suppressive effects of paeonol treatment on the cell colony formation and migration. Not only that, paeonol significantly reduced the number of invasive PCa cells (**Figure 5F**) and notably increased the cell apoptosis rate (**Figure 5G**), whereas silencing of miR-145-5p or GOLM1 overexpression was both able to attenuate the anti-tumor effects of paeonol. The above findings suggested that paeonol inhibits PCa cell colony formation, migration, invasion and promotes apoptosis via modulating the miR-145-5p/GOLM1 axis.

miR-145-5p inhibition attenuated the in vivo antitumor effect of paeonol and was accompanied by altered GOLM1 expression

Compared with inhibitor NC group, miR-145-5p was significantly down-regulated in tumor tissues of nude mice injected with LNCaP cells transfected with miR-145-5p inhibitor (**Figure 6A**). From the 6th day of administration, the paeonol group showed a notable decrease in tumor volume; while silencing of miR-145-5p reduced the tumor suppressive effect of paeonol, resulting in an increase in tumor volume (**Figure 6B**). After 14 d of continuous administration, the tumor weight of the paeonol group was significantly reduced, while silencing of miR-145-5p significantly attenuated this inhibitory effect of paeonol, leading to a notable increase in tumor weight (**Figure 6C**, **6D**). Through TUNEL staining, we found that paeonol injection led to a notable rise in the number of TUNEL-positive cells, indicating that paeonol promoted apoptosis of PCa cells; while silencing of miR-145-5p decreased TUNEL-positive cells (**Figure 6E**). After paeonol administration, immunohistochemical findings demonstrated that Ki67 level in PCa tissues was markedly decreased, which indicated that paeonol inhibited cell proliferation; but silencing of miR-145-5p caused Ki67 levels to increase again (**Figure 6F**). In line with the *in vitro* results, paeonol markedly increased miR-145-5p level and down-regulated GOLM1 in tumor tissues, and this regulatory effect was markedly attenuated by miR-145-5p silencing (**Figure 6G**, **6H**). These findings suggested that miR-145-5p inhibition attenuated the *in vivo* antitumor effect of paeonol and was accompanied by altered GOLM1 expression.

Discussion

The focus on herbal extracts and their ability to halt the progression of tumors has received widespread attention in recent years. Paeonol exhibits a range of pharmacological effects. Liu *et al*. noticed that paeonol induced cycle arrest of colorectal cancer cells, reduced cell proliferation, and stimulated apoptosis [32]. In the current research, we identified that paeonol decreased the viability of PCa cells, inhibited their colony formation, migration and invasion, and induced apoptosis. Not only that, paeonol also showed efficient anti-tumor activity in nude mice tumors, confirmed that paeonol might be a new therapeutic option for managing PCa.

miRNAs are known to be crucial in the progression of tumors, participating in key processes including cell proliferation, migration, differentiation and tumor angiogenesis [33-35]. miR-145-5p expression is downregulated in a range of cancer types, such as breast [36], ovarian [37], and colorectal [38] cancers, and it is widely recognized as a tumor suppressor miRNA. The findings of Sun *et al*. revealed that miR-145-5p overexpression caused PCa cell cycle arrest, induced apoptosis, and functioned as a cancer suppressor gene [39]. In this work, compared to normal cells, miR-145-5p expression was downregulated in PCa cells, aligning with previous research findings. Notably, paeonol treatment up-regulated miR-145-5p expression. Additionally, miR-145-5p overexpression also suppressed colony formation, reduced cell migration and invasive abilities, and promoted apoptosis, providing evidence that paeonol might play an anti-tumor role by increasing miR-145-5p level. It is worth noting that wound healing assay and Transwell assay are only used to evaluate the migration and invasion phenotypes of cells *in vitro*, and cannot directly represent the metastasis of tumors *in vivo*.

Binding of miRNAs to target genes leads to degradation or inhibition of translation of target mRNAs, thus exerting a regulatory effect on tar-

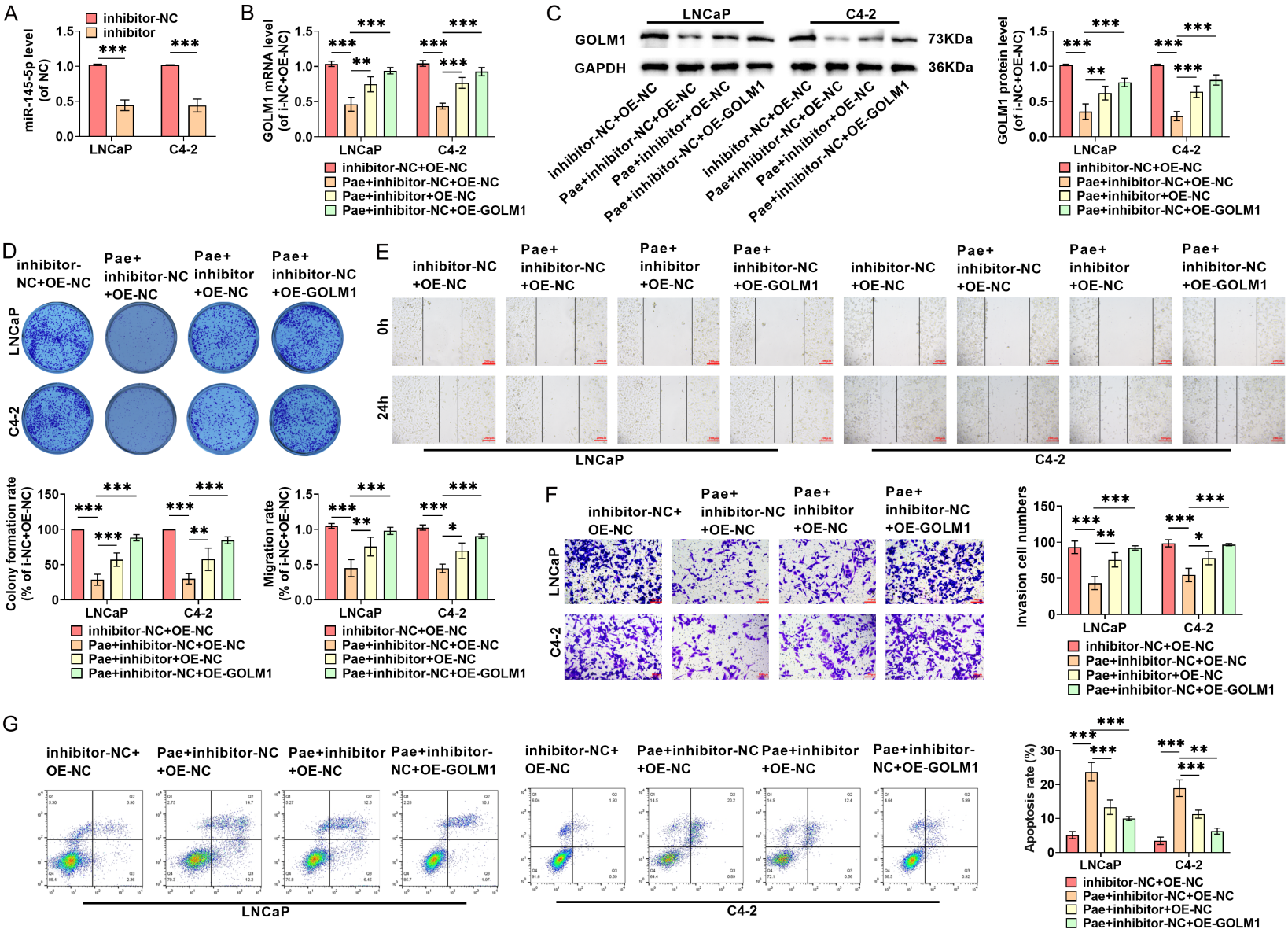

Figure 5. Paeonol inhibits malignant phenotypes of PCa cells by modulating the miR-145-5p/GOLM1 axis. A. qRT-PCR was performed to quantify the level of miR-145-5p after transfection with inhibitor NC or inhibitor to verify the transfection efficiency. B, C. The GOLM1 level in LNCaP and C4-2 cells after paeonol treatment

was examined using qRT-PCR and Western blot. D. Colony formation assay was used to evaluate the impact of paeonol on cell proliferative ability after silencing of miR-145-5p or GOLM1 overexpression. E. The cell migration after paeonol treatment was assessed by wound healing assay (10×, 200 μm). F. Transwell assays were performed to examine the influence of silencing of miR-145-5p or GOLM1 overexpression after paeonol treatment on the number of invasive cells (20×, 100 μm). G. Apoptosis rates were detected by flow cytometry after paeonol treatment with miR-145-5p silencing or GOLM1 overexpression. PCa: Prostate Cancer; GOLM1: Golgi Membrane Protein 1; qRT-PCR: Quantitative Real-Time Polymerase Chain Reaction. (*P<0.05, **P<0.01, ***P<0.001).

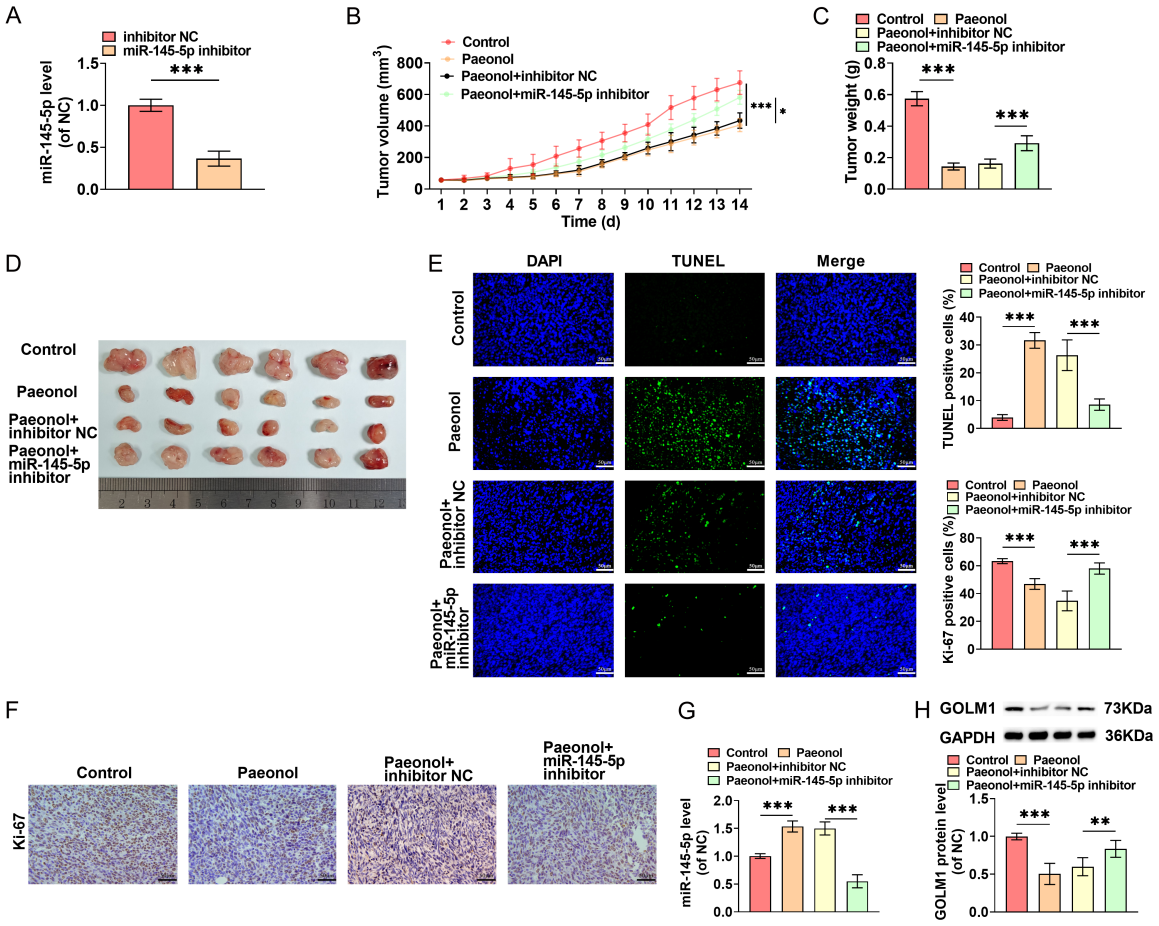

Figure 6. Paeonol suppresses tumor growth *in vivo*. (A) qRT-PCR was performed to detect the transfection efficiency of miR-145-5p inhibitor or inhibitor NC. (B) Tumor volume was measured daily to evaluate tumor growth. After the last administration, nude mice were humanely euthanized under anesthesia, and the tumors were excised and weighed (C), and photographed for documentation (D). (E) TUNEL staining was performed to detectcell apoptosis in tumor tissues, and the rate of TUNEL-positive cells was quantified (40×, 50 μm). (F) Immunohistochemistry assay was performed to detect Ki-67 expression in tumor tissues (40×, 50 μm). (G) qRT-PCR was performed to detect miR-145-5p level in tumor tissues. (H) Western blotting was performed to detect the protein expression level of GOLM1. qRT-PCR: Quantitative Real-Time Polymerase Chain Reaction; TUNEL: Terminal Deoxynucleotidyl Transferase dUTP Nick End Labeling; GOLM1: Golgi Membrane Protein 1. (*P<0.05, **P<0.01, ***P<0.001).

get mRNAs [40]. A single miRNA can target numerous downstream genes, and multiple miRNAs can influence a single gene. This intricate regulatory network can control the expression of multiple genes using one miRNA or finely tune the expression of a gene with a combination of multiple miRNAs [41]. Therefore, we postulated that miR-145-5p could potentially exert anti-tumor properties through regulating downstream target genes. Using miRWalk, miRDB and GEPIA databases, we predicted that GOLM1 was a downstream target gene of miR-145-5p.

GOLM1, a transmembrane protein expressed primarily in epithelial cells, plays a critical role

in promoting the invasion and metastasis of tumor cells [42]. According to Guan *et al*., GOLM1 showed high levels in ovarian cancer patients and this elevated expression was linked to unfavorable prognosis [43]. Furthermore, GOLM1 overexpression activates the AKT/glycogen synthase kinase 3β pathway, leading to increased invasive and metastatic capacities of colorectal cancer cells [44]. These research findings point to GOLM1 playing a role as an oncogene across various cancer types. In our research, there was a marked elevation in GOLM1 expression in PCa cells in contrast to normal cells, in line with the findings of the GEPIA database. miR-145-5p overexpression evidently decreased GOLM1 level, confirming that miR-145-5p directly targets and negatively regulates GOLM1. GOLM1 overexpression reversed the suppression of miR-145-5p overexpression on the PCa progression. Furthermore, paeonol treatment downregulated GOLM1 in PCa cells and tissues, whereas silencing of miR-145-5p partially attenuated the anti-tumor effects of paeonol and accompanied by obvious GOLM1 upregulation. *In vivo* data indicated that the anti-tumor action of paeonol was closely correlated with the modulation of the miR-145-5p/GOLM1 axis.

This study has certain limitations. We mainly explored the downstream mechanism by which paeonol suppresses PCa progression via the miR-145-5p/GOLM1 axis *in vitro*. Due to the absence of *in vivo* GOLM1 overexpression rescue experiments, the causal relationship of this regulatory axis in animal models cannot be fully defined. We have not yet investigated whether the elevation of miR-145-5p induced by paeonol stems from transcriptional activation, epigenetic modification, altered miRNA processing and maturation, or enhanced RNA stability. Additionally, we did not establish an *in vivo* metastasis model in this research, and only verified the anti-migration and anti-invasion effects of paeonol through *in vitro* functional assays. In subsequent studies, we will systematically explore the upstream molecular mechanism of paeonol regulating miR-145-5p expression from the perspectives of transcriptional regulation, epigenetic modification and non-coding RNA processing, to complete the full regulatory network of paeonol against PCa. Meanwhile, the anti-metastatic potential of paeonol could be further verified using orthotopic transplantation metastasis models or experimental metastasis models.

Conclusion

Through up-regulating miR-145-5p and down-regulating GOLM1, paeonol suppresses cell viability, migratory and invasive phenotypes, and induces apoptosis in PCa cells. In the subcutaneous xenograft model, paeonol also exhibited prominent anti-tumor effects, which was closely associated with the modulation of the miR-145-5p/GOLM1 axis. This research uncovered the action mechanism of paeonol in inhibiting the malignant progression of PCa by *in vitro* cellular experiments and subcutaneous xenograft tumor model, and provided new references for the clinical application of paeonol.

Disclosure of conflict of interest

None.

Abbreviations

PCa, Prostate cancer; miRNA, microRNA; GOLM1, Golgi membrane protein 1; WT, wild type; MUT, mutant type.

Address correspondence to: Yingxin Zhang, College of Life and Environmental Sciences, Minzu University of China, No. 27, South Zhongguancun Street, Haidian District, Beijing 100081, China. E-mail: yingxin2005zhang@hotmail.com

References

[1] Kratzer TB, Mazzitelli N, Star J, Dahut WL, Jemal A and Siegel RL. Prostate cancer statistics, 2025. CA Cancer J Clin 2025; 75: 485-497.

[2] Rosellini M, Santoni M, Mollica V, Rizzo A, Cimadamore A, Scarpelli M, Storti N, Battelli N, Montironi R and Massari F. Treating prostate cancer by antibody-drug conjugates. Int J Mol Sci 2021; 22: 1551.

[3] Siegel RL, Miller KD, Wagle NS and Jemal A. Cancer statistics, 2023. CA Cancer J Clin 2023; 73: 17-48.

[4] Schaeffer EM, Srinivas S, Adra N, An Y, Barocas D, Bitting R, Bryce A, Chapin B, Cheng HH, D'Amico AV, Desai N, Dorff T, Eastham JA, Farrington TA, Gao X, Gupta S, Guzzo T, Ippolito JE, Kuettel MR, Lang JM, Lotan T, McKay RR, Morgan T, Netto G, Pow-Sang JM, Reiter R, Roach M, Robin T, Rosenfeld S, Shabsigh A, Spratt D, Teply BA, Tward J, Valicenti R, Wong

JK, Shead DA, Snedeker J and Freedman-Cass DA. Prostate cancer, version 4.2023, NCCN clinical practice guidelines in oncology. J Natl Compr Canc Netw 2023; 21: 1067-1096.
[5] Simon NI, Parker C, Hope TA and Paller CJ. Best approaches and updates for prostate cancer biochemical recurrence. Am Soc Clin Oncol Educ Book 2022; 42: 1-8.
[6] Desai K, McManus JM and Sharifi N. Hormonal therapy for prostate cancer. Endocr Rev 2021; 42: 354-373.
[7] Yamada Y and Beltran H. The treatment landscape of metastatic prostate cancer. Cancer Lett 2021; 519: 20-29.
[8] Rebello RJ, Oing C, Knudsen KE, Loeb S, Johnson DC, Reiter RE, Gillessen S, Van der Kwast T and Bristow RG. Prostate cancer. Nat Rev Dis Primers 2021; 7: 9.
[9] Cai M, Song XL, Li XA, Chen M, Guo J, Yang DH, Chen Z and Zhao SC. Current therapy and drug resistance in metastatic castration-resistant prostate cancer. Drug Resist Updat 2023; 68: 100962.
[10] Sharma KK, Gupta S and Bisen PS. Enhancing gastrointestinal (GI) cancer therapies with ganoderma lucidum: a review of mechanisms and efficacy. Journal of Cancer Biomoleculars and Therapeutics 2025; 2: 15-44.
[11] Beeraka NM, Nagalakshmi A, Satyavathi A, Kote DM, Reddy Y P, Basappa B, Nikolenko VN, Bannimath G, Bulygin KV and P A M. Ginsenoside Rh4 suppresses notch3 and PI3K/Akt pathway to inhibit growth and metastasis of gastric cancer cells. Journal of Cancer Biomoleculars and Therapeutics 2025; 2: 145-156.
[12] Wu R, Liu Y, Zhang F, Dai S, Xue X, Peng C, Li Y and Li Y. Protective mechanism of Paeonol on central nervous system. Phytother Res 2024; 38: 470-488.
[13] Liu H and Zhang C. Paeonol induces antitumor effects in hepatocellular carcinoma cells through survivin via the cyclooxygenase-2/prostaglandin E2 signaling pathway. Transl Cancer Res 2020; 9: 7183-7195.
[14] Wu M, Yu Z, Li X, Zhang X, Wang S, Yang S, Hu L and Liu L. Paeonol for the treatment of atherosclerotic cardiovascular disease: a pharmacological and mechanistic overview. Front Cardiovasc Med 2021; 8: 690116.
[15] Lv J, Zhu S, Chen H, Xu Y, Su Q, Yu G and Ma W. Paeonol inhibits human lung cancer cell viability and metastasis in vitro via miR-126-5p/ZEB2 axis. Drug Dev Res 2022; 83: 432-446.
[16] Cheng CS, Chen JX, Tang J, Geng YW, Zheng L, Lv LL, Chen LY and Chen Z. Paeonol inhibits pancreatic cancer cell migration and invasion through the inhibition of TGF-β1/Smad signaling and epithelial-mesenchymal-transition. Cancer Manag Res 2020; 12: 641-651.
[17] Chen XM, Jia CL and Zhu ZY. Paeonol impacts ovarian cancer cell proliferation, migration, invasion and apoptosis via modulating the transforming growth factor beta/smad3 signaling pathway. J Physiol Pharmacol 2023; 74.
[18] Wang S, Yang S, Yang X, Deng D, Li J and Dong M. Research progress of traditional chinese medicine monomers in reversing multidrug resistance of breast cancer. Am J Chin Med 2023; 51: 575-594.
[19] Li M, Cai O, Yu Y and Tan S. Paeonol inhibits the malignancy of Apatinib-resistant gastric cancer cells via LINC00665/miR-665/MAPK1 axis. Phytomedicine 2022; 96: 153903.
[20] Du J, Song D, Li J, Li Y, Li B and Li L. Paeonol triggers apoptosis in HeLa cervical cancer cells: the role of mitochondria-related caspase pathway. Psychopharmacology (Berl) 2022; 239: 2083-2092.
[21] Conti I, Varano G, Simioni C, Laface I, Milani D, Rimondi E and Neri LM. miRNAs as influencers of cell-cell communication in tumor microenvironment. Cells 2020; 9: 220.
[22] Macvanin M, Obradovic M, Zafirovic S, Stanimirovic J and Isenovic ER. The role of miRNAs in metabolic diseases. Curr Med Chem 2023; 30: 1922-1944.
[23] He B, Zhao Z, Cai Q, Zhang Y, Zhang P, Shi S, Xie H, Peng X, Yin W, Tao Y and Wang X. miRNA-based biomarkers, therapies, and resistance in cancer. Int J Biol Sci 2020; 16: 2628-2647.
[24] Menon A, Abd-Aziz N, Khalid K, Poh CL and Naidu R. miRNA: a promising therapeutic target in cancer. Int J Mol Sci 2022; 23: 11502.
[25] Kadkhoda S and Ghafouri-Fard S. Function of miRNA-145-5p in the pathogenesis of human disorders. Pathol Res Pract 2022; 231: 153780.
[26] Ge J, Zhang Z, Shao G, Wei D, Tang B, Shi Z, Zou R and Wang X. miR-145-5p modulates CDCA3 to overcome gemcitabine resistance in pancreatic cancer. Gen Physiol Biophys 2025; 44: 175-183.
[27] Chen X, Li D, Su Q, Ling X, Ding S, Xu R, Liu Z, Qin Y, Zhang J, Yang Z, Kang X, Qi Y and Wu H. MicroRNA-145-5p inhibits the tumorigenesis of breast cancer through SENP2-regulated ubiquitination of ERK2. Cell Mol Life Sci 2024; 81: 461.
[28] Luo B, Yuan Y, Zhu Y, Liang S, Dong R, Hou J, Li P, Xing Y, Lu Z, Lo R and Kuang GM. microRNA-145-5p inhibits prostate cancer bone metastatic by modulating the epithelial-mesenchymal transition. Front Oncol 2022; 12: 988794.
[29] Yan J, Zhou B, Li H, Guo L and Ye Q. Recent advances of GOLM1 in hepatocellular carcinoma. Hepat Oncol 2020; 7: Hep22.
[30] Qin X, Liu L, Li Y, Luo H, Chen H and Weng X. GOLM1 promotes epithelial-mesenchymal

transition by activating TGFβ1/Smad2 signaling in prostate cancer. Technol Cancer Res Treat 2023; 22: 15330338231153618.
[31] Zhang L, Chen WX, Li LL, Cao YZ, Geng YD, Feng XJ, Wang AY, Chen ZL, Lu Y and Shen AZ. Paeonol suppresses proliferation and motility of non-small-cell lung cancer cells by disrupting STAT3/NF-κB signaling. Front Pharmacol 2020; 11: 572616.
[32] Liu LH, Shi RJ and Chen ZC. Paeonol exerts anti-tumor activity against colorectal cancer cells by inducing G0/G1 phase arrest and cell apoptosis via inhibiting the Wnt/β-catenin signaling pathway. Int J Mol Med 2020; 46: 675-684.
[33] Hill M and Tran N. miRNA interplay: mechanisms and consequences in cancer. Dis Model Mech 2021; 14: dmm047662.
[34] Ali Syeda Z, Langden SSS, Munkhzul C, Lee M and Song SJ. Regulatory mechanism of MicroRNA expression in cancer. Int J Mol Sci 2020; 21: 1723.
[35] Ashrafizadeh M. Cell death mechanisms in human cancers: molecular pathways, therapy resistance and therapeutic perspective. Journal of Cancer Biomoleculars and Therapeutics 2024; 1: 17-40.
[36] Rajarajan D, Kaur B, Penta D, Natesh J and Meeran SM. miR-145-5p as a predictive biomarker for breast cancer stemness by computational clinical investigation. Comput Biol Med 2021; 135: 104601.
[37] Pan Y, Huang Q, Peng X, Yu S and Liu N. Circ_0015756 promotes ovarian cancer progression via the miR-145-5p/PSAT1 axis. Reprod Biol 2022; 22: 100702.
[38] Chen Q, Zhou L, Ye X, Tao M and Wu J. miR-145-5p suppresses proliferation, metastasis and EMT of colorectal cancer by targeting CDCA3. Pathol Res Pract 2020; 216: 152872.
[39] Sun J, Deng L and Gong Y. MiR-145-5p inhibits the invasion of prostate cancer and induces apoptosis by inhibiting WIP1. J Oncol 2021; 2021: 4412705.
[40] Hussen BM, Hidayat HJ, Salihi A, Sabir DK, Taheri M and Ghafouri-Fard S. MicroRNA: a signature for cancer progression. Biomed Pharmacother 2021; 138: 111528.
[41] Peng W, Wu R, Dai W, Ning Y, Fu X, Liu L and Liu L. MiRNA-gene network embedding for predicting cancer driver genes. Brief Funct Genomics 2023; 22: 341-350.
[42] Chen J, Lin Z, Liu L, Zhang R, Geng Y, Fan M, Zhu W, Lu M, Lu L, Jia H, Zhang J and Qin LX. GOLM1 exacerbates CD8(+) T cell suppression in hepatocellular carcinoma by promoting exosomal PD-L1 transport into tumor-associated macrophages. Signal Transduct Target Ther 2021; 6: 397.
[43] Guan J, Qin Y, Deng G and Zhao H. GOLM1 as a potential therapeutic target modulates B7-H3 secretion to drive ovarian cancer metastasis. Evid Based Complement Alternat Med 2022; 2022: 5151065.
[44] Mao Z, Wu Y, Yao P and Xing C. GOLM1 facilitates human colorectal cancer progression and metastasis via activating the AKT/GSK3β/EMT axis. Neoplasma 2023; 70: 136-144.